Journal of Membrane Science 460 (2014) 206–212

Contents lists available at ScienceDirect

Journal of Membrane Science

journal homepage: www.elsevier.com/locate/memsci

# Combined organic and colloidal fouling in forward osmosis: Fouling reversibility and the role of applied pressure

Yeowon Kim [a], Menachem Elimelech [b], Ho Kyong Shon [c], Seungkwan Hong [a,*]

[a] School of Civil, Environmental & Architectural Engineering, Korea University, 1-5 Ga, Anam-Dong, Seongbuk-Gu, Seoul 136-713, Republic of Korea
[b] Department of Chemical and Environmental Engineering, Yale University, New Haven, Connecticut 06520-8286, USA
[c] School of Civil and Environmental Engineering, University of Technology, Sydney (UTS), Post Box 129, Broadway, NSW 2007, Australia

ARTICLE INFO

*Article history:*
Received 23 September 2013
Received in revised form
12 February 2014
Accepted 25 February 2014
Available online 4 March 2014

*Keywords:*
Forward osmosis
Combined organic and colloidal fouling
Alginate fouling
Silica fouling
Fouling reversibility

ABSTRACT

In this study, we systematically investigated the propensity and reversibility of combined organic–colloidal fouling in forward osmosis (FO) under various solution chemistries (pH and calcium ion concentrations) and applied hydraulic pressure on the feed side. Alginate, silica colloids, and their mixture (i.e., combined organic–colloidal) were used as model foulants. Our findings demonstrate that combined organic–colloidal foulants caused more rapid flux decline than the individual foulants due to the synergistic effect of alginate and silica colloids. As a result, much lower flux recovery was achieved by physical cleaning induced by increasing the cross-flow rate, in contrast to single foulants of which the fouling layer was easily removed under all solution conditions. Interestingly, less flux decline was observed at neutral pH for combined fouling, while acidic conditions were favorable for alginate fouling and basic solutions caused more silica fouling, thereby providing clear evidence for the combined fouling effect. It was also found that calcium ions enhanced water flux decline and induced the formation of less reversible combined organic–colloidal fouling layers. Lastly, the role of applied hydraulic pressure on the feed side in FO was examined to elucidate the mechanism of fouling layer formation, fouling reversibility, and water flux recovery. Higher fouling propensity and lower fouling reversibility of combined organic–colloidal fouling were observed in the presence of applied hydraulic pressure on the feed side. This observation suggests that the lower fouling propensity and greater fouling reversibility in FO compared to reverse osmosis (RO), are attributable to unpressurized operating conditions in FO.



## 1. Introduction

Water shortages and depletion of fresh water supplies, likely exacerbated by climate change, place a great demand for alternative water resources. The urgent need for securing high quality water supply from unconventional sources, such as seawater and wastewater, has resulted in the emergence of advanced membrane technologies. Compared with thermal driven desalination, membrane processes based on reverse osmosis (RO) technology are much more energy efficient, with a global market of RO desalination increasing by more than 10% annually [1]. Despite the major advancements in RO desalination technology, its efficiency and sustainable operation are hampered by the relatively high energy consumption [2]. To reduce energy demand and costs, innovative system designs, such as multi-stage seawater reverse osmosis (SWRO) [2–5], energy saving processes that can utilize low grade heat [4,6], and new membrane processes, including forward osmosis (FO) [1,7,8], have been suggested.

Forward osmosis has recently attracted heightened attention due to the wide range of prospective applications in desalination and wastewater reuse. Unlike the hydraulic pressure-driven RO process, water flux in FO is driven by osmosis due to a concentration difference between the feed water and a concentrated draw solution [7,9]. The apparent advantages of FO technology stem from its operation without applied hydraulic pressure, which has the potential for lower capital and operation costs [7,9–12]. The lack of applied hydraulic pressure on the feed side in FO has also been proposed as beneficial for fouling control compared to pressure-driven membrane processes [7,9,12–16].

Membrane fouling is a major obstruction in many membrane applications, which compromises process efficiency and increases operation and maintenance costs [17–20]. Several research efforts have been made to clarify the FO fouling mechanisms for expanding FO applications. Organic fouling behavior in FO was studied and compared to that in RO, demonstrating that under identical physicochemical conditions, more flux decline was generally

* Corresponding author. Tel.: +822 329 033 22; fax: +822 928 7656.
*E-mail address:* skhong21@korea.ac.kr (S. Hong).

http://dx.doi.org/10.1016/j.memsci.2014.02.038
0376-7388 

observed in FO compared to RO due to cake-enhanced osmotic pressure that was accelerated by reverse permeation of draw solution [14]. However, higher operating cross-flow velocity was able to restore the initial flux by removing FO fouling layer, while such improvement was not observed in RO because of the compact fouling layer [14]. A more recent study investigated colloidal fouling in FO focusing on the role of reverse salt diffusion [21]. Similar to organic fouling, colloidal fouling induced elevated salt concentration near the membrane surface at feed side, primarily due to reverse salt flux from the draw to the feed side, which resulted in significant reduced water flux. However, in the absence of particle destabilization by increased salt concentration, the colloidal fouling layer was reversible upon increasing the cross-flow rate [21].

Although significant efforts have been made to understand fouling phenomena in FO, fundamental studies on fouling reversibility under various feed chemical compositions are rather limited. Particularly, there are no fundamental studies which investigate the role of hydraulic pressure in fouling, which is one of the most important factors discriminating fouling mechanisms between FO and RO. The main objective of this study was to evaluate the fouling propensity and reversibility of FO with a mixture of organic and colloidal foulants. Specifically, the mechanisms of combined organic and colloidal fouling were elucidated by examining the effects of individual foulants as well as synergistic effects with the combined organic and colloidal foulants. We have placed special emphasis on the role of osmotic pressure in fouling and fouling reversibility in FO compared to the role of hydraulic pressure in RO, which has been an issue of great interest in the literature. By designing fouling experiments in FO with increasing applied pressures on the feed side while maintaining the initial water flux at a fixed value, we clearly showed that osmotic pressure driving force results in more reversible fouling layers compared to hydraulic pressure driving force.

## 2. Materials and methods

### 2.1. FO membrane

A commercially available cellulose triacetate (CA) membrane from Hydration Technology Innovations (Albany, OR, USA) was used in this study. Membrane samples were stored in deionized (DI) water at 4 °C and then soaked in DI water at room temperature for 24 h before each experiment. For each fouling test, a fresh membrane sample was cut and placed into a bench-scale cross-flow membrane test cell in the typical FO mode (i.e., active layer faces feed solution). The total thickness of the membrane is approximately 50 μm and other membrane properties are described elsewhere [21].

### 2.2. Organic and colloidal foulants

Two different types of model foulants, organic (alginate macromolecules) and inorganic (silica colloids), were used to study combined organic–colloidal fouling in FO. The model foulants represent polysaccharides and suspended colloidal matter, respectively, which are commonly found in real feed waters. We have used sodium alginate (12–80 kDa) as a model hydrophilic organic foulant (Sigma-Aldrich, St. Louis, MO, USA). For fouling experiments, alginate was added to the feed solution from a concentrated (2 g/L) sodium alginate stock solution. The concentration of alginate in the fouling experiments was 100 mg/L. Silica ($SiO_2$) colloids were selected as a model particulate foulant. Silica colloids were added to the feed solution from a stock suspension (ST-ZL, Nissan Chemical Industries, Ltd., Japan). For fouling experiments, the concentration of silica colloids in the feed solution was 1 g/L. According to information from the manufacturer, the approximate size of the colloidal particles is 100 nm. The particles were prepared as a stable concentrated aqueous suspension at an alkaline pH of 8.5–9.5. Colloidal particles of the required concentration were dispersed in deionized water (DI) with conductivity of less than 1 μS/cm. Prior to use, the stock suspension was stirred vigorously for 10 min for uniform dispersion of the colloidal particles.

The model foulants were examined individually, and then, their mixture at a certain ratio was investigated in fouling experiments under different feed solution chemistries (i.e., pH and calcium ion concentration). For meaningful comparison of the fouling runs, similar hydrodynamic conditions (i.e., 7 μm/s initial water flux and 8.61 cm/s cross-flow velocity) and feed solution chemistries were employed for all experiments.

### 2.3. FO lab-scale test unit

Experiments were performed in two different lab-scale membrane test units to investigate the fouling propensity and reversibility in FO. The first FO membrane test unit consisted of a monomer-cast (MC) nylon flow cell, two reservoirs for feed and draw solutions, two variable speed gear pumps (Cole-Parmer, Vernon Hills, IL) for circulation of each solution, a digital scale for measurement of permeate water mass, two customized salt-resistant Teflon flow meters, and a thermostatic bath. The various components of the unit were connected with Teflon tubing. A schematic diagram and detailed description of the FO system are given elsewhere [22].

The second FO unit was specially designed for application of hydraulic pressure on the membrane feed side (Fig. 1). An identical variable speed gear pump was used for the circulation of the draw solution as a typical FO system, but a high pressure pump replaced the gear pump on the feed side to apply hydraulic pressure. To prevent membrane breakage by the applied pressure, several layers of tailored permeate carriers obtained from commercial flat-sheet RO membrane modules (Hydranautics Inc., U.S.) were inserted as spacers on both sides of cell channel. These spacers are porous enough to allow flow of the solutions, and firm enough to bear the direct impact of pressure on the membrane surface. The dimensions of the feed and draw solution channels in both FO units were 77 mm long, 26 mm wide, and 3 mm deep.

### 2.4. Fouling tests

Fouling and cleaning experiments were conducted with the bench-scale membrane cross-flow units described above. The first

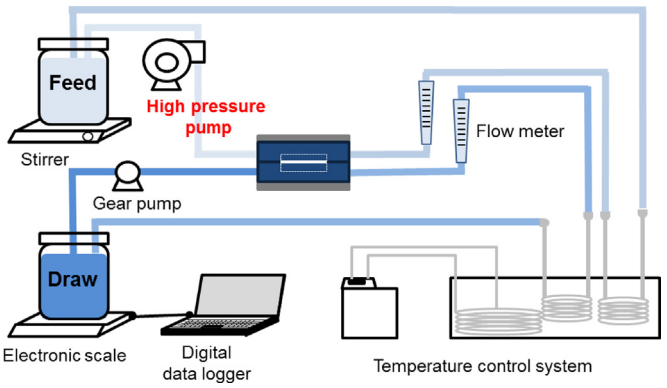


**Fig. 1.** Schematic description of the cross-flow FO membrane test unit specially designed for applying hydraulic pressure on the feed side of the membrane in order to investigate the impact of applied hydraulic pressure on fouling in FO.

set of experiments was performed with the typical FO system using a 5 M NaCl draw solution. Each fouling run was performed for 3 h at a cross-flow velocity of 8.61 cm/s, followed by 1 h of simple physical washing at an increased cross-flow velocity (four-fold) of 34.44 cm/s. After cleaning, the cross-flow velocity was reduced to its initial level, and water flux recovered was determined to assess the fouling reversibility. Data was corrected for the dilution of draw solution by the permeate water flux based on a baseline FO run.

In order to examine the effect of applied hydraulic pressure on fouling behavior, various pressures were applied on the feed side and results were compared with those obtained with the unpressurized FO fouling runs. All experiments were performed in FO mode (i.e., active layer faces feed solution), but with additional hydraulic pressure applied on the feed side. Permeate flux was continuously monitored using a digital balance and recorded every 3 min for the entire period of each experiment.

## 3. Results and discussion

### 3.1. Combined organic–colloidal fouling behavior under various solution chemistries

Fouling experiments with combined organic–colloidal foulants were carried out to elucidate FO fouling behavior under various solution chemistries. Specifically, combined fouling behavior was examined with a mixture of alginate and silica colloids to study whether synergistic effects exist between these different types of foulants. Relatively high concentrations of organic and colloidal foulants were used to accelerate the fouling rate. The total ionic strength of feed solution was kept identical to maintain constant osmotic pressure and initial water flux in all fouling experiments. Fouling run duration was 5 h, which was sufficient enough to observe fouling and flux recovery behaviors.

#### 3.1.1. Effect of solution pH

Fig. 2 shows flux decline and recovery under combined organic–colloidal fouling at various feed solution pH. Overall, when both alginate and silica colloids were present in the feed solution, a rapid flux decline occurred, even at the very beginning of the fouling runs. The rapid flux decline for combined fouling suggests synergistic effects between organic and colloidal fouling

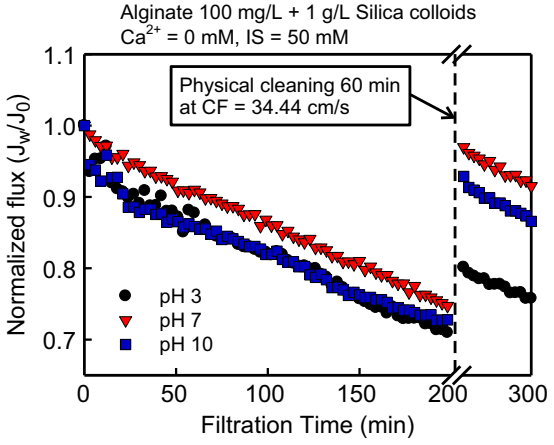


**Fig. 2.** Representative flux decline curves and fouling reversibility after physical cleaning for combined organic–colloidal fouling at various feed solution pH. Experimental conditions were as follows: 5 M NaCl draw solution, feed solution with 100 mg/L sodium alginate and 1 g/L of silica colloids, and feed solution ionic strength of 50 mM NaCl. Temperatures of both feed and draw solutions were 25 ± 1 °C and cross-flow rate was 8.61 cm/s during the fouling period and increased to 34.44 cm/s for physical cleaning.

**Table 1**
The effect of solution pH on the extent of flux decline (presented as the relative water flux at the end of the fouling experiment) and demonstration of synergistic effect in combined organic–colloidal fouling. The numbers represent the decrease amount of flux ($J_w/J_0$).

| pH | Organic | Colloid | Organic+colloid (calculated) | Organic+colloid combined (experimental) | Exp.–cal. |
|---|---|---|---|---|---|
| 3 | 0.113 | 0.079 | 0.192 | 0.260 | 0.068 |
| 7 | 0.076 | 0.096 | 0.172 | 0.237 | 0.065 |
| 10 | 0.049 | 0.124 | 0.173 | 0.272 | 0.099 |

[23–25]. In other words, the effect of the co-existence of these two types of foulants on flux decline was greater than the algebraic sum of their individual effects [23], as presented in Table 1. The extent of flux decline (i.e., $J_w/J_0$ at the end of the fouling run) of combined organic–colloidal fouling was greater than the calculated sum of the single organic and colloidal fouling, with the difference ranging from 0.068 to 0.099.

To examine FO fouling reversibility by physical cleaning (hydraulic cleaning), 1 h of cleaning at a much higher crossflow rate (34.44 cm/s) was performed after all fouling experiments. Overall, as shown in Fig. 2, the permeate water flux was recovered to some degree at the solution pH values investigated. However, the effectiveness of physical cleaning varied for each feed solution pH, with the lowest flux recovered at acidic conditions (pH 3) and the highest flux recovered at pH 7.

Each representative single foulant (alginate or silica colloids) was examined to reveal its own fouling behavior dependence on solution pH and to explain the fundamental mechanisms of combined organic–colloidal fouling. The effect of solution pH on single organic fouling (i.e., alginate alone) is presented in Fig. 3a, showing less water flux decline at higher solution pH. This behavior is ascribed to the reduction of electrostatic repulsion among alginate macromolecules and/or between alginate and the membrane surface at lower pH. The alginate macromolecules are protonated at an acidic solution and are thus neutrally charged. This induces more alginate deposition and accumulation on the membrane surface, which results in severe fouling [26]. At pH 7 and 10, the flux decline was not substantial, which could be explained by a looser and less substantial fouling layer due to the increased electrostatic repulsion among negatively charged alginate macromolecules [20,26].

Feed solution pH, however, did not affect the reversibility of the organic fouling layer (Fig. 3a), showing complete flux recovery in all cases. Moreover, the flux recovered by physical cleaning appeared even slightly higher than the initial flux as indicated by $J_w/J_0$ values greater than 1, likely due to hydrophilization of the membrane by alginate. After the formation of the organic fouling layer, NaCl diffusing from the draw solution to the fouling layer on the feed side accelerated the cake enhanced osmotic pressure (CEOP) phenomenon (referred to as accelerated CEOP or A-CEOP), which resulted in severe flux decline [14]. When the foulants were washed away by the hydrodynamic shear force during the physical cleaning, the fouling layer and CEOP vanished, and as a result, the flux was fully recovered.

In colloidal fouling, the high salt concentration near the membrane surface, particularly caused by the reverse diffusion of draw salt, made silica colloids very unstable in the alkaline solution (pH 10, Fig. 3b), which decreased particle–particle interaction and enhanced silica particle deposition on the membrane surface [18,21,27]. Regardless of feed solution pH, however, the colloidal fouling layer was readily removed by simple physical cleaning as with the single organic fouling.

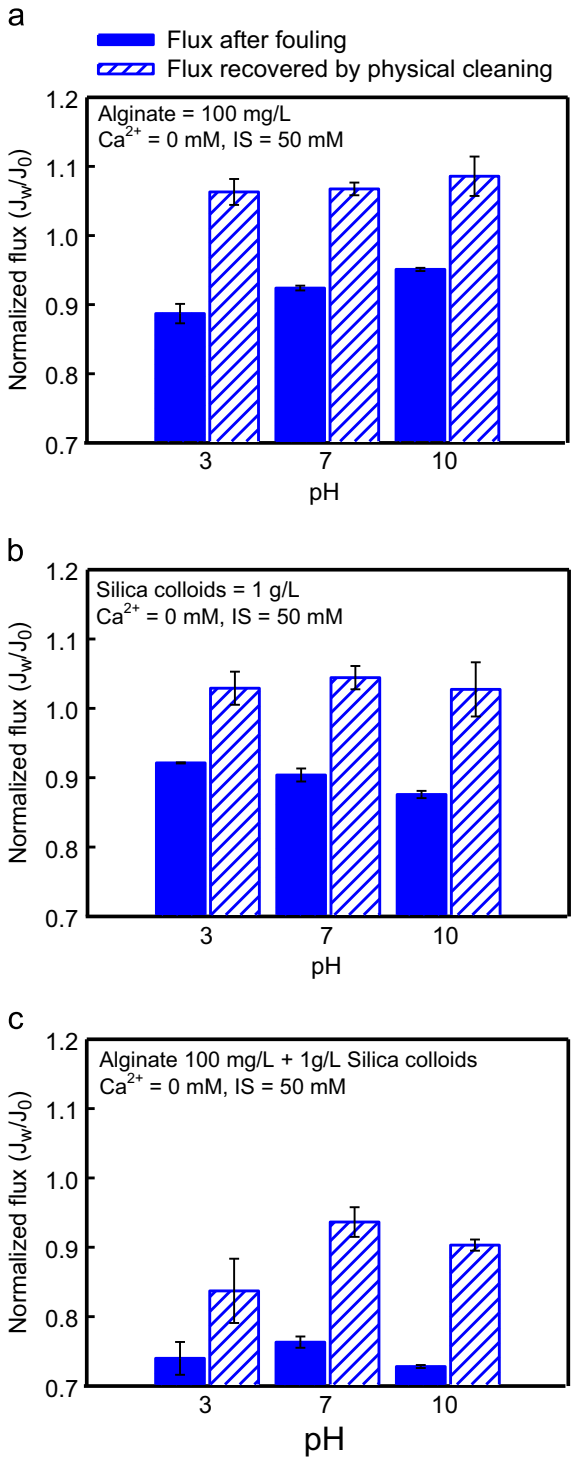


**Fig. 3.** Fouling propensity (presented as relative flux after fouling) and reversibility (presented as relative flux after physical cleaning) in FO under various pH conditions for: (a) 100 mg/L alginate, (b) 1 g/L of silica colloids, and (c) combined organic–colloidal foulants (mixture of 100 mg/L of alginate and 1 g/L of silica colloid). Other experimental conditions are similar to those described in Fig. 2.

We note that because of the opposite fouling behavior of alginate and colloidal fouling with respect to solution pH, flux decline by combined organic–colloidal fouling was minimal at neutral pH as shown in Fig. 3c. The acidic feed solution (i.e., pH 3) was favorable to alginate fouling, but not to colloid aggregation and deposition. On the other hand, the alkaline solution (i.e., pH 10) made silica colloids more unstable and formed a thick colloidal fouling layer, but had the opposite effect on alginate. The

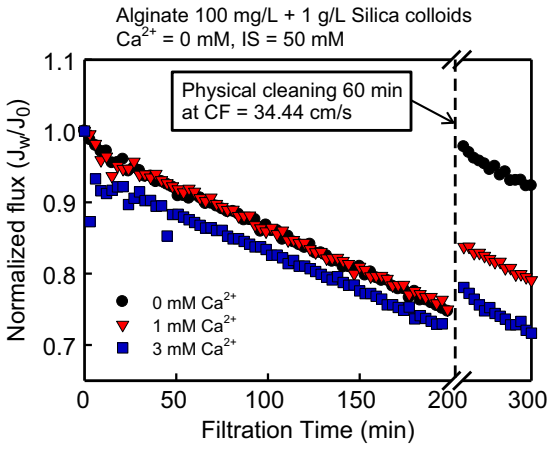


**Fig. 4.** Representative flux decline curves and fouling reversibility after physical cleaning for combined organic–colloidal fouling at various calcium ion concentrations at pH 7. Experimental conditions were as follows: 5 M NaCl draw solution, feed solution with 100 mg/L sodium alginate and 1 g/L of silica colloids, and feed solution ionic strength of 50 mM NaCl. Temperatures of both feed and draw solutions were 25 ± 1 °C and cross-flow rate was 8.61 cm/s during the fouling period and increased to 34.44 cm/s for physical cleaning.

**Table 2**
The effect of calcium ion concentration on the extent of flux decline (presented as the relative water flux at the end of the fouling experiment) and demonstration of synergistic effect in combined organic–colloidal fouling.

| $Ca^{2+}$ (mM) | Organic | Colloid | Organic+colloid (calculated) | Organic+colloid combined (experimental) | Exp.–cal. |
|---|---|---|---|---|---|
| 0 | 0.060 | 0.096 | 0.156 | 0.237 | 0.081 |
| 1 | 0.074 | 0.123 | 0.197 | 0.256 | 0.059 |
| 3 | 0.091 | 0.148 | 0.239 | 0.276 | 0.037 |

reversibility of combined organic–colloidal fouling by physical cleaning was also most effective at pH 7. The flux after cleaning was recovered up to 93.6% at pH 7, while lower recoveries of 83.7% and 90.3% were observed at pH 3 and pH 10, respectively. The synergistic effects of combined organic–colloidal fouling are clearly demonstrated when examining fouling reversibility, as individual foulants (alginate or silica colloids) exhibited complete flux recovery (Fig. 3a and b), but this was not the case for the mixture of these foulants (Fig. 3c).

### 3.1.2. *Effect of $Ca^{2+}$ concentration*

The normalized water flux profiles for combined organic–colloidal fouling at increasing $Ca^{2+}$ concentrations are shown in Fig. 4, indicating that higher $Ca^{2+}$ concentrations caused more significant flux decline. Synergistic effects of alginate and silica colloids in combined organic–colloidal fouling were also observed in the presence of calcium ions. As summarized in Table 2, combined organic–colloidal fouling resulted in more flux decline than the algebraic sum of individual organic and colloidal fouling. The difference between experimental (observed) and calculated (sum of individual organic and colloidal) ranged from 0.081 to 0.037. Further, as Fig. 4 indicates, the presence of $Ca^{2+}$ ions in the feed solution in combined fouling also appears to inhibit flux recovery by physical cleaning.

The collective effects of calcium ions in combined organic–colloidal fouling are compared with single organic and colloidal fouling in Fig. 5. As expected, for alginate alone, higher $Ca^{2+}$ concentration in the feed solution caused more flux decline (Fig. 5a). This intensified flux decline in the presence of $Ca^{2+}$ is

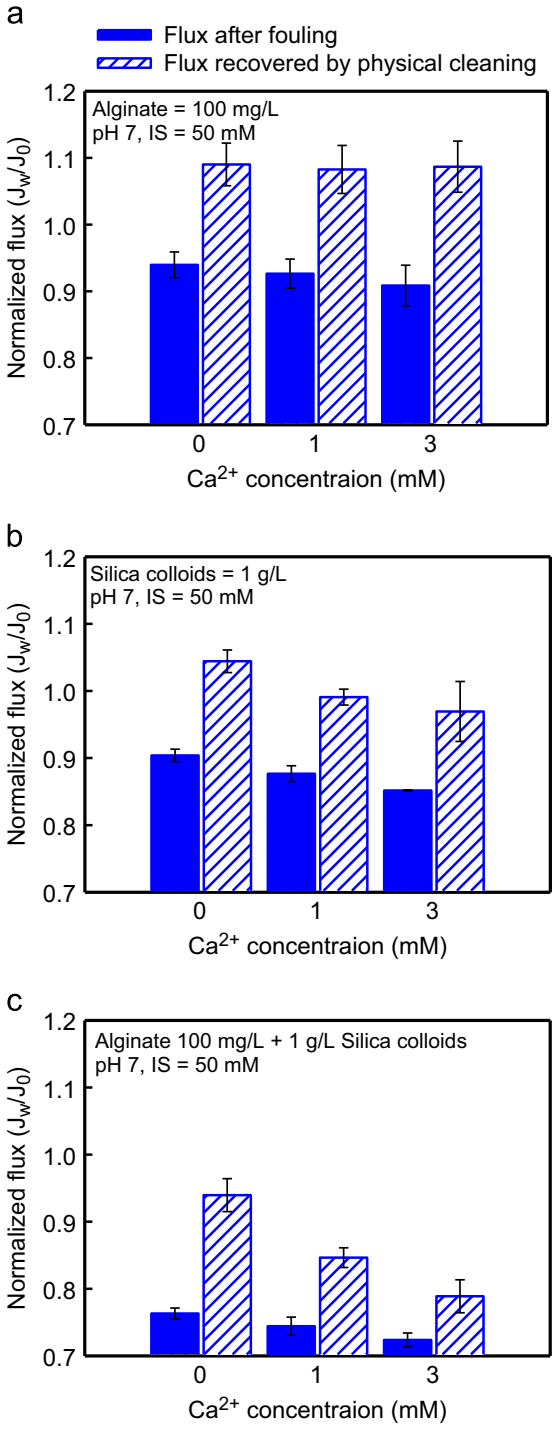


**Fig. 5.** Fouling propensity (presented as relative flux after fouling) and reversibility (presented as relative flux after physical cleaning) in FO at various calcium ion concentrations at pH 7 for: (a) 100 mg/L alginate, (b) 1 g/L of silica colloids, and (c) combined organic-colloidal foulants (mixture of 100 mg/L of alginate and 1 g/L of silica colloid). Other experimental conditions are similar to those described in Fig. 4.

attributed to intermolecular bridging by complexation among alginate molecules, resulting in the formation of a cross-linked alginate gel layer on the membrane surface [16,20,22,28]. However, this gel layer was not strong enough to resist the hydrodynamic shear forces during physical cleaning as complete flux recovery was observed (Fig. 5a). For colloidal fouling alone (Fig. 5b), $Ca^{2+}$ also caused higher flux decline by destabilizing the colloidal particles more effectively [21,29–31]. The colloidal fouling layer was reversible by simple physical cleaning, although slightly lower recoveries were obtained in the presence of calcium compared to the case with no calcium.

The effect of $Ca^{2+}$ on combined organic–colloidal fouling reflected the trend of single organic and colloidal fouling behaviors, with fouling much more pronounced for the mixture of these foulants. However, the impact of $Ca^{2+}$ on the reversibility of combined fouling was much more dramatic than that on the fouling behavior. Flux recovery was greatly diminished in the presence of calcium due to strong binding between alginate and colloidal silica manifested by $Ca^{2+}$ (Fig. 5c). The results from this study strongly suggest that $Ca^{2+}$ plays a critical role in the formation of irreversible organic–colloidal fouling and that synergistic effects between organic and colloidal foulants are the key for controlling fouling reversibility.

### 3.2. Combined organic–colloidal fouling behavior in the presence of hydraulic pressure

The fouling behavior in FO was observed in the presence of applied hydraulic pressure on the feed side in order to fundamentally investigate the apparent superior fouling reversibility in FO compared to RO and to unravel the role of hydraulic versus osmotic pressure in fouling. We first studied fouling behavior under identical bulk osmotic pressure differences (i.e., the same draw solution concentration), but with varying hydraulic pressures applied to the feed water side. Next, we carried out fouling experiments at the same initial water flux by adjusting the draw solution concentration for each experiment at different applied hydraulic pressure.

Physical cleaning was conducted after the fouling runs to investigate the effect of hydraulic pressure on fouling layer reversibility. In such experiments, the feed side was pressurized during the 3 h of the combined organic–colloidal fouling FO run, and then pressure was released for 1 h of physical cleaning induced by high cross-flow velocity. By performing a series of such experiments, the role of hydraulic pressure was critically delineated, and the implications for understanding the propensity and reversibility of FO fouling was fundamentally discussed.

#### 3.2.1. Fouling at a fixed draw solution concentration and varying hydraulic pressure

Fig. 6 presents the extent of flux decline (i.e., $J_w/J_0$ at the end of the fouling run) and the relative water flux after physical cleaning for experiments carried out at various applied hydraulic pressures (at a fixed draw solution concentration) for combined organic–colloidal fouling. Overall, fouling was more severe and fouling layer became less reversible when hydraulic pressure was applied on the feed side. When no hydraulic pressure was applied on the feed side (i.e., typical FO operation), water flux was reduced to 93.1% of its initial value after 3 h of fouling. When hydraulic pressure increased to 6.9 and 17.3 bar, the water flux was further reduced to 91.8% and 89.8% of the corresponding initial water fluxes, respectively. As we discussed later, this observation is attributed to compression of the deformable organic foulants by the applied hydraulic pressure.

The impact of applied hydraulic pressure on fouling reversibility and subsequent water flux recovery was quite remarkable. While the water flux with no hydraulic pressure on the feed side was recovered up to 95.2% of its initial flux after cleaning, the results obtained under applied pressures (6.9 and 17.3 bar) showed no fouling reversibility, implying that hydraulic pressure impacts the fouling layer structure. However, one might argue that this observation is due the higher initial water flux and consequently greater permeation drag when operating at higher applied

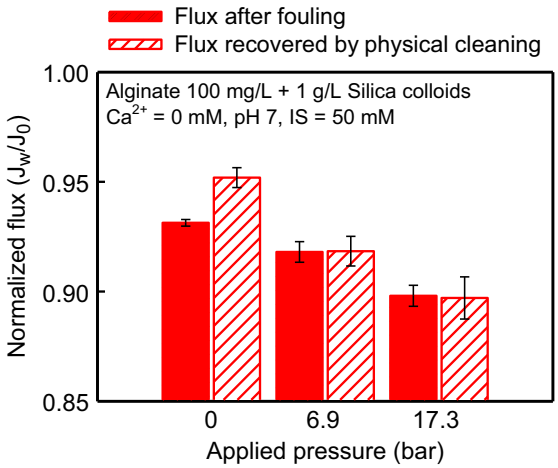


**Fig. 6.** Fouling propensity (presented as relative flux after fouling) and reversibility (presented as relative flux after physical cleaning) in FO under various applied hydraulic pressures and fixed draw solution concentration (5 M NaCl). Experimental conditions were as follows: feed solution with 100 mg/L sodium alginate and 1 g/L of silica colloids, and feed solution ionic strength of 50 mM NaCl. Temperatures of both feed and draw solutions were $20 \pm 1$ °C and cross-flow rate was 8.61 cm/s during the fouling period and increased to 34.44 cm/s for physical cleaning. Solution pH was adjusted to pH 7.

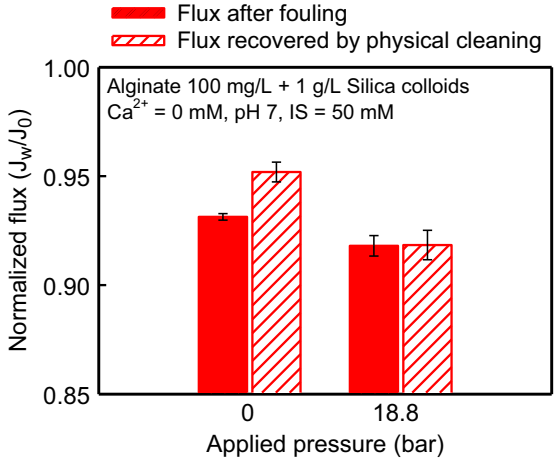


**Fig. 7.** Fouling propensity (presented as relative flux after fouling) and reversibility (presented as relative flux after physical cleaning) in FO at zero and 18.8 bar applied hydraulic pressure on the feed solution side and a fixed initial water flux of 7.0 μm/s (25.34 L $m^{-2}$ $h^{-1}$). To obtain this initial water flux, a 5 M of NaCl draw solution was used for run without pressure and 3.5 M of NaCl draw solution for 18.8 bar applied pressure. Other experimental conditions were as follows: feed solution with 100 mg/L sodium alginate and 1 g/L of silica colloids, and feed solution ionic strength of 50 mM NaCl. Temperatures of both feed and draw solutions were $20 \pm 1$ °C and cross-flow rate was 8.61 cm/s during the fouling period and increased to 34.44 cm/s for physical cleaning. Solution pH was adjusted to pH 7.

hydraulic pressure but fixed draw solution concentration [32–34]. To address this possibility, we carried out fouling experiments at identical initial water flux but increased hydraulic pressure as discussed in the following section.

### 3.2.2. *Fouling at the same initial water flux and varying hydraulic pressures*

The effect of applied hydraulic pressures on combined organic–colloidal fouling at an identical initial water flux is shown in Fig. 7. An initial water flux of 7.0 μm/s (25.34 L $m^{-2}$ $h^{-1}$) was employed in these fouling runs. We have used a 5 M of NaCl draw solution to achieve this initial water flux when no hydraulic pressure was applied (i.e., typical FO operation), while a draw solution of 3.5 M NaCl was used to attain the same initial water flux when a pressure of 18.8 bar was applied to the feed side. Fouling was more significant at an applied pressure 18.8 bar compared to the case with no applied pressure. Because the initial water flux was identical in both experiments, the greater flux decline with applied pressure is attributed to the formation of a more compact fouling layer under the action of hydraulic pressure. The impact on physical cleaning is even more striking. While physical cleaning was effective in recovering a portion of the lost water flux when no pressure was applied, no flux recovery was observed after fouling experiments at an applied pressure of 18.8 bar. These results imply that increasing cross-flow during the cleaning period is not sufficient to remove the compact and cohesive fouling layer that was formed under applied hydraulic pressure.

### 3.3. *Implications for fouling behavior of FO compared to RO*

In the previous sections, we described the results of a series of fouling experiments which were carried with and without applied hydraulic pressure. Part of the motivation of these studies was to better understand the difference between the structures of organic–colloidal fouling layers formed in FO compared to RO. In FO, the driving force for permeate water flux is the osmotic pressure difference between the draw and feed solutions. The RO process, on the other hand, is operated under highly pressurized conditions depending on feed water osmotic pressure. Our results suggest that in a non-pressurized FO membrane system, foulants that accumulate on the membrane surface form a relatively loose, reversible fouling layer that can be washed away by simple physical cleaning, except at high calcium ion concentration. However, organic–colloidal fouling layers formed under applied hydraulic pressures were not reversible, suggesting that more compact and cohesive fouling layers form in the presence of hydraulic pressure.

The proposed fouling layer structures for combined organic–colloidal fouling in FO and RO processes are schematically depicted in Fig. 8. The fouling layer structure in FO is mainly impacted by the permeation drag of the convective permeate flow induced by the osmotic pressure driving force, while in RO, in addition to the permeation drag, the applied hydraulic pressure compresses deformable organic molecules and the organic–colloidal clusters that accumulate on the membrane surface. Consequently, the fouling layer structure in FO is likely to be looser, sparser, and thicker than that in RO. Such loose and sparse fouling layers that form in FO could be reversible by simple physical cleaning induced by hydrodynamic shear [14,16,31]. On the other hand, fouling layers formed in RO are compact and more cohesive and will therefore be much less reversible, as indeed observed in our experiments under applied hydraulic pressure.

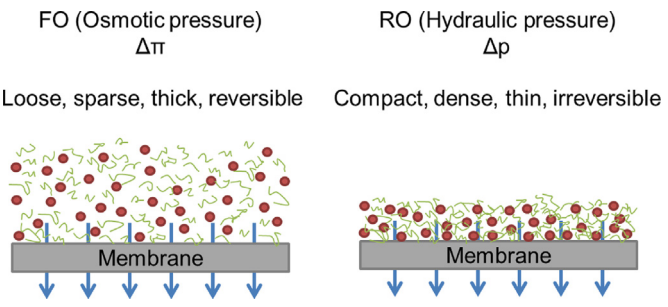


**Fig. 8.** Proposed combined fouling layer structure (i.e., with feed solution containing alginate and silica colloids) with and without applied hydraulic pressure.

## 4. Conclusion

Mechanisms and reversibility of combined organic–colloidal fouling in FO were systematically investigated under various solution chemistries and pressure conditions. Our results demonstrated synergistic effects for combined fouling with alginate and silica colloids, where overall flux decline was more severe with combined foulants compared to the sum of the individual contributions of alginate and silica colloids alone. We have also shown that the combined fouling behavior and synergistic effects are impacted by feed solution chemistry (i.e., pH and presence of calcium ions in the feed solution). The reversibility of combined organic–colloidal fouling was also investigated showing significant synergistic effects. While individual organic or colloidal fouling exhibited complete fouling reversibility in FO, combined organic–colloidal fouling exhibited a much lower reversibility, particularly in the presence of calcium ions in the feed solution. Our results also demonstrated that applied hydraulic pressure enhanced flux decline by forming a denser cake layer of organic molecules and colloids. Applied hydraulic pressure had also a marked impact on fouling reversibility. We have found that fouling layers formed during combined organic–colloidal fouling runs under applied hydraulic pressure were irreversible when subjected to physical cleaning by increasing the crossflow, while those formed in typical FO operation (i.e., no applied hydraulic pressure) were reversible to a large extent. These results suggest that operation under an osmotic pressure driving force (i.e., FO) results in less fouling and exhibits higher fouling reversibility compared to operation at hydraulic pressure driving force (i.e., RO). The impact of hydraulic pressure is attributed to the formation of more compact and dense fouling layer of the deformable organic foulants and organic–colloidal aggregates.

## Acknowledgments

This research was supported by the World Class University (WCU) program (Case III) through the National Research Foundation of Korea and funded by the Ministry of Education, Republic of Korea, (R33-10046) and partly by grant from the Fundamental R&D Program for Technology of World Premier Materials (WPM) funded by the Ministry of Trade, Industry and Energy, Republic of Korea.

## References

[1] M. Elimelech, W.A. Phillip, The future of seawater desalination: energy, technology, and the environment, Science 333 (2011) 712–717.
[2] C. Fritzmann, J. Löwenberg, T. Wintgens, T. Melin, State-of-the-art of reverse osmosis desalination, Desalination 216 (2007) 1–76.
[3] M. Li, Reducing specific energy consumption in Reverse Osmosis (RO) water desalination: an analysis from first principles, Desalination 276 (2011) 128–135.
[4] B. Peñate, L. García-Rodríguez, Current trends and future prospects in the design of seawater reverse osmosis desalination technology, Desalination 284 (2012) 1–8.
[5] T.Y. Cath, N.T. Hancock, C.D. Lundin, C. Hoppe-Jones, J.E. Drewes, A multi-barrier osmotic dilution process for simultaneous desalination and purification of impaired water, J. Membr. Sci. 362 (2010) 417–426.
[6] R.A. Tidball, R. Kadaj, Waste heat powered reverse osmosis plants, Desalination 39 (1981) 137–145.
[7] T. Cath, A. Childress, M. Elimelech, Forward osmosis: principles, applications, and recent developments, J. Membr. Sci. 281 (2006) 70–87.
[8] R.L. McGinnis, M. Elimelech, Global challenges in energy and water supply: the promise of engineered osmosis, Environ. Sci. Technol. 42 (2008) 8625–8629.
[9] L.A. Hoover, W.A. Phillip, A. Tiraferri, N.Y. Yip, M. Elimelech, Forward with osmosis: emerging applications for greater sustainability, Environ. Sci. Technol. 45 (2011) 9824–9830.
[10] J.R. McCutcheon, R.L. McGinnis, M. Elimelech, A novel ammonia–carbon dioxide forward (direct) osmosis desalination process, Desalination 174 (2005) 1–11.
[11] R.L. McGinnis, M. Elimelech, Energy requirements of ammonia–carbon dioxide forward osmosis desalination, Desalination 207 (2007) 370–382.
[12] S. Zhao, L. Zou, C.Y. Tang, D. Mulcahy, Recent developments in forward osmosis: opportunities and challenges, J. Membr. Sci. 396 (2012) 1–21.
[13] A. Achilli, T.Y. Cath, E.A. Marchand, A.E. Childress, The forward osmosis membrane bioreactor: a low fouling alternative to MBR processes, Desalination 239 (2009) 10–21.
[14] S. Lee, C. Boo, M. Elimelech, S. Hong, Comparison of fouling behavior in forward osmosis (FO) and reverse osmosis (RO), Jo. Membr. Sci. 365 (2010) 34–39.
[15] Z.-Y. Li, V. Yangali-Quintanilla, R. Valladares-Linares, Q. Li, T. Zhan, G. Amy, Flux patterns and membrane fouling propensity during desalination of seawater by forward osmosis, Water Res. 46 (2012) 195–204.
[16] B. Mi, M. Elimelech, Organic fouling of forward osmosis membranes: fouling reversibility and cleaning without chemical reagents, J. Membr. Sci. 348 (2010) 337–345.
[17] W.S. Ang, A. Tiraferri, K.L. Chen, M. Elimelech, Fouling and cleaning of RO membranes fouled by mixtures of organic foulants simulating wastewater effluent, J. Membr. Sci. 376 (2011) 196–206.
[18] M. Beyer, B. Lohrengel, L.D. Nghiem, Membrane fouling and chemical cleaning in water recycling applications, Desalination 250 (2010) 977–981.
[19] W. Guo, H.-H. Ngo, J. Li, A mini-review on membrane fouling, Bioresour. Technol. 122 (2012) 27–34.
[20] S. Hong, M. Elimelech, Chemical and physical aspects of natural organic matter (NOM) fouling of nanofiltration membranes, J. Membr. Sci. 132 (1997) 159–181.
[21] C. Boo, S. Lee, M. Elimelech, Z. Meng, S. Hong, Colloidal fouling in forward osmosis: Role of reverse salt diffusion, J. Membr. Sci. 390–391 (2012) 277–284.
[22] B. Mi, M. Elimelech, Chemical and physical aspects of organic fouling of forward osmosis membranes, J. Membr. Sci. 320 (2008) 292–302.
[23] Y. Liu, B. Mi, Combined fouling of forward osmosis membranes: synergistic foulant interaction and direct observation of fouling layer formation, J. Membr. Sci. 407–408 (2012) 136–144.
[24] S. Lee, J. Cho, M. Elimelech, Combined influence of natural organic matter (NOM) and colloidal particles on nanofiltration membrane fouling, J. Membr. Sci. 262 (2005) 27–41.
[25] Q. Li, M. Elimelech, Synergistic effects in combined fouling of a loose nanofiltration membrane by colloidal materials and natural organic matter, J. Membr. Sci. 278 (2006) 72–82.
[26] S. Lee, W.S. Ang, M. Elimelech, Fouling of reverse osmosis membranes by hydrophilic organic matter: implications for water reuse, Desalination 187 (2006) 313–321.
[27] G. Singh, L. Song, Impact of feed water acidification with weak and strong acids on colloidal silica fouling in ultrafiltration membrane processes, Water Res. 42 (2008) 707–713.
[28] Y. Mo, K. Xiao, Y. Shen, X. Huang, A new perspective on the effect of complexation between calcium and alginate on fouling during nanofiltration, Sep. Purif. Technol. 82 (2011) 121–127.
[29] C.Y. Tang, T.H. Chong, A.G. Fane, Colloidal interactions and fouling of NF and RO membranes: a review, Adv. Colloid Interface Sci. 164 (2011) 126–143.
[30] T. Koo, Y.J. Lee, R. Sheikholeslami, Silica fouling and cleaning of reverse osmosis membranes, Desalination 139 (2001) 43–56.
[31] B. Mi, M. Elimelech, Silica scaling and scaling reversibility in forward osmosis, Desalination (2012).
[32] J.R. McCutcheon, M. Elimelech, Influence of concentrative and dilutive internal concentration polarization on flux behavior in forward osmosis, J. Membr. Sci. 284 (2006) 237–247.
[33] Q. Li, Z. Xu, I. Pinnau, Fouling of reverse osmosis membranes by biopolymers in wastewater secondary effluent: role of membrane surface properties and initial permeate flux, J. Membr. Sci. 290 (2007) 173–181.
[34] X. Zhu, M. Elimelech, Colloidal fouling of reverse osmosis membranes: measurements and fouling mechanisms, Environ. Sci. Technol. 31 (1997) 3654–3662.